

Intrinsic finite element modeling of a linear membrane shell problem

Peter Hansbo ^{*} Mats G. Larson [†]

Abstract

A Galerkin finite element method for the membrane elasticity problem on a meshed surface is constructed by using two-dimensional elements extended into three dimensions. The membrane finite element model is established using the intrinsic approach suggested by Delfour and Zolésio [8].

1 Introduction

Models of thin-shell structures are often established using differential geometry to define the governing differential equations in two dimensions, cf. Ciarlet [4] for an overview. A simpler approach is the classical engineering trick of viewing the shell as an assembly of flat elements, in which simple transformations of the two-dimensional stiffness matrices are performed, cf., e.g., Zienkiewicz [15]. In contrast to these approaches, Delfour and Zolesio [8, 9, 10] established elasticity models on surfaces using the signed distance function, which can be used to describe the geometric properties of a surface. In particular, the intrinsic tangential derivatives were used for modeling purposes as the main differential geometric tool and the partial differential equations were established in three dimensions. A similar concept had been used earlier in a finite element setting for the numerical discretization of the Laplace-Beltrami operator on surfaces by Dziuk [12], resulting in a remarkably clean and simple implementation. For diffusion-like problems, the intrinsic approach has become the focal point of recent research on numerical solutions of problems posed on surfaces, cf., e.g., [1, 2, 7, 11, 13, 14]

The purpose of this paper is to begin to explore the possibilities of the intrinsic approach in finite element modeling of thin-shell structures, focusing on the simplest model, that of the membrane shell without bending stiffness. We derive a membrane model using the intrinsic framework and generalize the finite element approach of [12]. Finally, we give some elementary numerical examples.

^{*}Department of Mechanical Engineering, Jönköping University, SE-55111 Jönköping, Sweden.

[†]Department of Mathematics and Mathematical Statistics, Umeå University, SE-90187 Umeå, Sweden

2 The membrane shell model problem

2.1 Basic notation

We begin by recalling the fundamentals of the approach of Delfour and Zolesio [8, 9, 10]. Let Σ be a smooth two-dimensional surface imbedded in \mathbb{R}^3 , with outward pointing normal \mathbf{n} . If we denote the signed distance function relative to Σ by $d(\mathbf{x})$, for $\mathbf{x} \in \mathbb{R}^3$, fulfilling $\nabla d = \mathbf{n}$, we can define the domain occupied by the membrane by

$$\Omega_t = \{\mathbf{x} \in \mathbb{R}^3 : |d(\mathbf{x})| < t/2\},$$

where t is the thickness of the membrane. The closest point projection $\mathbf{p} : \Omega_t \rightarrow \Sigma$ is given by

$$\mathbf{p}(\mathbf{x}) = \mathbf{x} - d(\mathbf{x})\mathbf{n}(\mathbf{x}),$$

the Jacobian matrix of which is

$$\nabla \mathbf{p} = \mathbf{I} - d\nabla \otimes \mathbf{n} - \mathbf{n} \otimes \mathbf{n}$$

where \mathbf{I} is the identity and \otimes denotes exterior product. The corresponding linear projector $\mathbf{P}_\Sigma = \mathbf{P}_\Sigma(\mathbf{x})$, onto the tangent plane of Σ at $\mathbf{x} \in \Sigma$, is given by

$$\mathbf{P}_\Sigma := \mathbf{I} - \mathbf{n} \otimes \mathbf{n},$$

and we can then define the surface gradient ∇_Σ as

$$\nabla_\Sigma := \mathbf{P}_\Sigma \nabla. \tag{2.1}$$

The surface gradient thus has three components, which we shall denote by

$$\nabla_\Sigma =: \begin{bmatrix} \frac{\partial}{\partial x_1^\Sigma} \\ \frac{\partial}{\partial x_2^\Sigma} \\ \frac{\partial}{\partial x_3^\Sigma} \end{bmatrix}.$$

For a vector valued function $\mathbf{v}(\mathbf{x})$, we define the tangential Jacobian matrix as

$$\nabla_\Sigma \otimes \mathbf{v} := \begin{bmatrix} \frac{\partial v_1}{\partial x_1^\Sigma} & \frac{\partial v_1}{\partial x_2^\Sigma} & \frac{\partial v_1}{\partial x_3^\Sigma} \\ \frac{\partial v_2}{\partial x_1^\Sigma} & \frac{\partial v_2}{\partial x_2^\Sigma} & \frac{\partial v_2}{\partial x_3^\Sigma} \\ \frac{\partial v_3}{\partial x_1^\Sigma} & \frac{\partial v_3}{\partial x_2^\Sigma} & \frac{\partial v_3}{\partial x_3^\Sigma} \end{bmatrix}$$

and the surface divergence $\nabla_\Sigma \cdot \mathbf{v} := \text{tr} \nabla_\Sigma \otimes \mathbf{v}$.

2.2 The surface strain and stress tensors

We next define a surface strain tensor

$$\boldsymbol{\varepsilon}_\Sigma(\mathbf{u}) := \frac{1}{2} (\nabla_\Sigma \otimes \mathbf{u} + (\nabla_\Sigma \otimes \mathbf{u})^\top),$$

which is extensively used in [8, 9, 10], where it is employed to derive models of shells based on purely mathematical arguments.

From a mechanical point of view, the problem of using $\boldsymbol{\varepsilon}_\Sigma(\mathbf{u})$ as a fundamental measure of strain on a surface lies in it not being an in-plane tensor, in that $\boldsymbol{\varepsilon}_\Sigma(\mathbf{u}) \cdot \mathbf{n} \neq \mathbf{0}$. The shear strains associated with the out-of-plane direction are typically neglected in mechanical models, but are present in $\boldsymbol{\varepsilon}_\Sigma(\mathbf{u})$ (cf. Remark 2.1). To obtain an in-plane strain tensor we need to use the projection twice to define

$$\boldsymbol{\varepsilon}_\Sigma^P(\mathbf{u}) := \mathbf{P}_\Sigma \boldsymbol{\varepsilon}(\mathbf{u}) \mathbf{P}_\Sigma,$$

which lacks all out-of-plane strain components. For a shell, where plane stress is assumed, this strain tensor can still be used, since out-of-plane strains do not contribute to the strain energy.

Remark 2.1 *It is instructive to work out the details at a surface point whose surrounding is tangential to the x_1x_2 -plane. In this case $\mathbf{n} = (0, 0, 1)$,*

$$\mathbf{P}_\Sigma = \begin{bmatrix} 1 & 0 & 0 \\ 0 & 1 & 0 \\ 0 & 0 & 0 \end{bmatrix}, \quad \nabla_\Sigma \otimes \mathbf{u} = \begin{bmatrix} \frac{\partial u_1}{\partial x_1} & \frac{\partial u_2}{\partial x_1} & \frac{\partial u_3}{\partial x_1} \\ \frac{\partial u_1}{\partial x_2} & \frac{\partial u_2}{\partial x_2} & \frac{\partial u_3}{\partial x_2} \\ 0 & 0 & 0 \end{bmatrix},$$

$$\boldsymbol{\varepsilon}_\Sigma(\mathbf{u}) = \begin{bmatrix} \frac{\partial u_1}{\partial x_1} & \frac{1}{2} \left(\frac{\partial u_1}{\partial x_2} + \frac{\partial u_2}{\partial x_1} \right) & \frac{1}{2} \frac{\partial u_3}{\partial x_1} \\ \frac{1}{2} \left(\frac{\partial u_1}{\partial x_2} + \frac{\partial u_2}{\partial x_1} \right) & \frac{\partial u_2}{\partial x_2} & \frac{1}{2} \frac{\partial u_3}{\partial x_2} \\ \frac{1}{2} \frac{\partial u_3}{\partial x_1} & \frac{1}{2} \frac{\partial u_3}{\partial x_2} & 0 \end{bmatrix},$$

and

$$\boldsymbol{\varepsilon}_\Sigma^P = \begin{bmatrix} \frac{\partial u_1}{\partial x_1} & \frac{1}{2} \left(\frac{\partial u_1}{\partial x_2} + \frac{\partial u_2}{\partial x_1} \right) & 0 \\ \frac{1}{2} \left(\frac{\partial u_1}{\partial x_2} + \frac{\partial u_2}{\partial x_1} \right) & \frac{\partial u_2}{\partial x_2} & 0 \\ 0 & 0 & 0 \end{bmatrix}.$$

The terms in $\boldsymbol{\varepsilon}_\Sigma$ not present in $\boldsymbol{\varepsilon}_\Sigma^P$ are shear strains that are typically neglected for thin structures, and it is clear that in our case $\boldsymbol{\varepsilon}_\Sigma^P$ is the relevant strain tensor.

However, the tensor $\boldsymbol{\varepsilon}_\Sigma^P$ is rather cumbersome to use directly in a numerical implementation; it would be much easier to work with $\boldsymbol{\varepsilon}_\Sigma$ which can be established using tangential derivatives. For this reason, we use the fact that there also holds (as is easily confirmed)

$$\boldsymbol{\varepsilon}_\Sigma^P(\mathbf{u}) = \mathbf{P}_\Sigma \boldsymbol{\varepsilon}_\Sigma(\mathbf{u}) \mathbf{P}_\Sigma = \frac{1}{2} (\mathbf{P}_\Sigma \nabla_\Sigma \otimes \mathbf{u} \mathbf{P}_\Sigma + (\mathbf{P}_\Sigma \nabla_\Sigma \otimes \mathbf{u} \mathbf{P}_\Sigma)^T),$$

and since $\mathbf{n} \cdot \boldsymbol{\varepsilon}_\Sigma(\mathbf{u}) \cdot \mathbf{n} = 0$ we have the following relation:

$$\boldsymbol{\varepsilon}_\Sigma^P(\mathbf{u}) = \boldsymbol{\varepsilon}_\Sigma(\mathbf{u}) - ((\boldsymbol{\varepsilon}_\Sigma(\mathbf{u}) \cdot \mathbf{n}) \otimes \mathbf{n} + \mathbf{n} \otimes (\boldsymbol{\varepsilon}_\Sigma(\mathbf{u}) \cdot \mathbf{n})),$$

so that, using dyadic double-dot product,

$$\boldsymbol{\sigma} : \mathbf{u} \otimes \mathbf{v} = (\boldsymbol{\sigma} \cdot \mathbf{u}) \cdot \mathbf{v}, \quad \mathbf{u} \otimes \mathbf{v} : \boldsymbol{\sigma} = \mathbf{u} \cdot (\mathbf{v} \cdot \boldsymbol{\sigma}),$$

where $\boldsymbol{\sigma}$ is a tensor and \mathbf{u}, \mathbf{v} are vectors, we arrive at

$$\boldsymbol{\varepsilon}_\Sigma^P(\mathbf{u}) : \boldsymbol{\varepsilon}_\Sigma^P(\mathbf{v}) = \boldsymbol{\varepsilon}_\Sigma(\mathbf{u}) : \boldsymbol{\varepsilon}_\Sigma(\mathbf{v}) - 2(\boldsymbol{\varepsilon}_\Sigma(\mathbf{u}) \cdot \mathbf{n}) \cdot (\boldsymbol{\varepsilon}_\Sigma(\mathbf{v}) \cdot \mathbf{n}), \quad (2.2)$$

which will be used in the finite element implementation below. We also note that there holds

$$\text{tr} \boldsymbol{\varepsilon}_\Sigma^P(\mathbf{v}) = \nabla_\Sigma \cdot \mathbf{v}, \quad (2.3)$$

where $\text{tr} \boldsymbol{\varepsilon} = \sum_k \varepsilon_{kk}$.

We shall assume an isotropic stress–strain relation,

$$\boldsymbol{\sigma} = 2\mu \boldsymbol{\varepsilon} + \lambda \text{tr} \boldsymbol{\varepsilon} \mathbf{I},$$

where $\boldsymbol{\sigma}$ is the stress tensor and \mathbf{I} is the identity tensor. The Lamé parameters λ and μ are related to Young’s modulus E and Poisson’s ratio ν via

$$\mu = \frac{E}{2(1+\nu)}, \quad \lambda = \frac{E\nu}{(1+\nu)(1-2\nu)}.$$

For the in-plane stress tensor we thus assume

$$\boldsymbol{\sigma}_\Sigma^P := 2\mu \boldsymbol{\varepsilon}_\Sigma^P + \lambda \text{tr} \boldsymbol{\varepsilon}_\Sigma^P \mathbf{P}_\Sigma,$$

in the plane strain case and, in the plane stress case, which is appropriate for a thin membrane,

$$\boldsymbol{\sigma}_\Sigma^P := 2\mu \boldsymbol{\varepsilon}_\Sigma^P + \lambda_0 \text{tr} \boldsymbol{\varepsilon}_\Sigma^P \mathbf{P}_\Sigma, \quad (2.4)$$

where

$$\lambda_0 := \frac{2\lambda\mu}{\lambda + 2\mu} = \frac{E\nu}{1 - \nu^2}.$$

2.3 The membrane shell equations

Consider a potential energy functional given by

$$\Pi(\mathbf{u}_t) := \frac{1}{2} \int_{\Omega_t} \boldsymbol{\sigma}(\mathbf{u}_t) : \boldsymbol{\varepsilon}(\mathbf{u}_t) d\Omega_t - \int_{\Omega_t} \mathbf{f}_t \cdot \mathbf{u}_t$$

where \mathbf{f}_t is of the form $\mathbf{f}_t = \mathbf{f} \circ \mathbf{p}$. Under the assumption of small thickness, we have

$$\int_{\Omega_t} f(\mathbf{x}) d\Omega_t \approx \int_{-t/2}^{t/2} \int_{\Sigma} f d\Sigma dz$$

and thus

$$\begin{aligned} \Pi(\mathbf{u}_t) &\approx \Pi_{\Sigma}^P(\mathbf{u}) := \frac{t}{2} \int_{\Sigma} \boldsymbol{\sigma}_{\Sigma}^P(\mathbf{u}) : \boldsymbol{\varepsilon}_{\Sigma}^P(\mathbf{u}) d\Sigma - t \int_{\Sigma} \mathbf{f} \cdot \mathbf{u} d\Sigma \\ &:= \frac{t}{2} (\boldsymbol{\sigma}_{\Sigma}^P(\mathbf{u}), \boldsymbol{\varepsilon}_{\Sigma}^P(\mathbf{u}))_{\Sigma} - t(\mathbf{f}, \mathbf{u})_{\Sigma}. \end{aligned}$$

Minimizing the potential energy leads to the variational problem of finding $\mathbf{u} \in V$, where V is an appropriate Hilbert space which we specify below, such that

$$a_{\Sigma}(\mathbf{u}, \mathbf{v}) = l_{\Sigma}(\mathbf{v}) \quad \forall \mathbf{v} \in V \quad (2.5)$$

where, by (2.2) and (2.3),

$$\begin{aligned} a_{\Sigma}(\mathbf{u}, \mathbf{v}) &= (2\mu \boldsymbol{\varepsilon}_{\Sigma}^P(\mathbf{u}), \boldsymbol{\varepsilon}_{\Sigma}^P(\mathbf{v}))_{\Sigma} + (\lambda_0 \operatorname{tr} \boldsymbol{\varepsilon}_{\Sigma}^P(\mathbf{u}), \operatorname{tr} \boldsymbol{\varepsilon}_{\Sigma}^P(\mathbf{v}))_{\Sigma} \\ &= (2\mu \boldsymbol{\varepsilon}_{\Sigma}(\mathbf{u}), \boldsymbol{\varepsilon}_{\Sigma}(\mathbf{v}))_{\Sigma} - (4\mu \boldsymbol{\varepsilon}_{\Sigma}(\mathbf{u}) \cdot \mathbf{n}, \boldsymbol{\varepsilon}_{\Sigma}(\mathbf{v}) \cdot \mathbf{n})_{\Sigma} + (\lambda_0 \nabla_{\Sigma} \cdot \mathbf{u}, \nabla_{\Sigma} \cdot \mathbf{v})_{\Sigma}, \end{aligned}$$

and $l_{\Sigma}(\mathbf{v}) = (\mathbf{f}, \mathbf{v})_{\Sigma}$. This variational problem formally coincides with the one analyzed in the classical differential geometric setting by Ciarlet and co-workers [6, 5], as shown in [10].

Splitting the displacement into a normal part $u_n := \mathbf{u} \cdot \mathbf{n}$ and a tangential part $\mathbf{u}_t := \mathbf{u} - u_n \mathbf{n}$ we have the identity

$$\boldsymbol{\varepsilon}_{\Sigma}^P(\mathbf{u}) = \boldsymbol{\varepsilon}_{\Sigma}^P(\mathbf{u}_t) + u_n \nabla \otimes \mathbf{n} = \boldsymbol{\varepsilon}_{\Sigma}^P(\mathbf{u}_t) + u_n \boldsymbol{\kappa},$$

where $\boldsymbol{\kappa} = \nabla \otimes \nabla d$ is the Hessian of the distance function d , cf. [10]. The bilinear form can therefore also be written in the form

$$\begin{aligned} a_{\Sigma}(\mathbf{u}, \mathbf{v}) &= (2\mu(\boldsymbol{\varepsilon}_{\Sigma}^P(\mathbf{u}_t) + u_n \boldsymbol{\kappa}), \boldsymbol{\varepsilon}_{\Sigma}^P(\mathbf{v}_t) + v_n \boldsymbol{\kappa})_{\Sigma} \\ &\quad + (\lambda_0(\operatorname{tr} \boldsymbol{\varepsilon}_{\Sigma}^P(\mathbf{u}_t) + u_n \operatorname{tr} \boldsymbol{\kappa}), \operatorname{tr} \boldsymbol{\varepsilon}_{\Sigma}^P(\mathbf{v}_t) + v_n \operatorname{tr} \boldsymbol{\kappa})_{\Sigma} \end{aligned} \quad (2.6)$$

This means that we do not have full ellipticity in our problem. Based on this observation we conclude that the natural function space for the variational formulation is

$$V = \{\mathbf{v} : v_n \in L_2(\Sigma) \quad \text{and} \quad \mathbf{v}_t \in [H^1(\Sigma)]^2\},$$

cf. [5]. The loss of ellipticity have consequences for the numerics and we comment on this in the numerical examples below.

Since

$$(\boldsymbol{\sigma}_\Sigma^P(\mathbf{u}), \boldsymbol{\varepsilon}_\Sigma^P(\mathbf{u}))_\Sigma = (\boldsymbol{\sigma}_\Sigma^P(\mathbf{u}), \boldsymbol{\varepsilon}_\Sigma(\mathbf{u}))_\Sigma$$

we find, using Green's formula, the pointwise equilibrium equation

$$-\nabla_\Sigma \cdot \boldsymbol{\sigma}_\Sigma^P(\mathbf{u}) = \mathbf{f} \quad \text{in } \Sigma, \quad (2.7)$$

which together with the constitutive law (2.4) defines the intrinsic differential equations of linear elasticity on surfaces.

3 The finite element method

3.1 Parametrization

Let $\mathcal{T}_h := \{T\}$ be a conforming, shape regular triangulation of Σ , resulting in a discrete surface Σ_h . We shall here consider an isoparametric parametrization of the surface (the same idea can however be used for arbitrary parametrizations). In the numerical examples below we use a piecewise linear approximation, meaning that the elements T will be planar. For the parametrization we wish to define a map $\mathbf{F} : (\xi, \eta) \rightarrow (x, y, z)$ from a reference triangle \hat{T} defined in a local coordinate system (ξ, η) to T , for all T . To this end, we write $\mathbf{x} = \mathbf{x}(\xi, \eta)$, where $\mathbf{x} = (x, y, z)$ are the physical coordinates on Σ_h . For any given parametrization, we can extend it outside the surface by defining

$$\mathbf{x}(\xi, \eta, \zeta) = \mathbf{x}(\xi, \eta) + \zeta \mathbf{n}(\xi, \eta)$$

where \mathbf{n} is the normal and $-t/2 \leq \zeta \leq t/2$. In some models, where the surface is an idealized thin structure, it is natural to think of t as a thickness.

For the representation of the geometry, we first introduce the following approximation of the normal:

$$\mathbf{n} \approx \mathbf{n}^h = \frac{\mathbf{n}_0^h}{|\mathbf{n}_0^h|}, \quad \mathbf{n}_0^h = \sum_i \mathbf{n}_i \varphi_i(\xi, \eta),$$

where $\varphi_i(\xi, \eta)$ are the finite element shape functions on the reference element (assumed linear in this paper), and \mathbf{n}_i denotes the normals in the nodes of the mesh. We then consider parametrizations of the type

$$\mathbf{x}(\xi, \eta, \zeta) \approx \mathbf{x}^h(\xi, \eta, \zeta) = \sum_i (\mathbf{x}_i \varphi_i(\xi, \eta) + \zeta \mathbf{n}_i \varphi_i(\xi, \eta)) \quad (3.1)$$

where \mathbf{x}_i are the physical location of the nodes on the surface. For the approximation of the solution, we use a constant extension,

$$\mathbf{u} \approx \mathbf{u}^h = \sum_i \mathbf{u}_i \varphi_i(\xi, \eta) \quad (3.2)$$

where \mathbf{u}_i are the nodal displacements, so that the finite element method is, in a sense, superparametric. Note that only the in-plane variation of the approximate solution will matter since we are looking at in-plane stresses and strains. We employ the usual finite element approximation of the physical derivatives of the chosen basis $\{\varphi_i\}$ on the surface, at (ξ, η) , as

$$\begin{bmatrix} \frac{\partial \varphi_j}{\partial x} \\ \frac{\partial \varphi_j}{\partial y} \\ \frac{\partial \varphi_j}{\partial z} \end{bmatrix} = \mathbf{J}^{-1}(\xi, \eta, 0) \begin{bmatrix} \frac{\partial \varphi_j}{\partial \xi} \\ \frac{\partial \varphi_j}{\partial \eta} \\ \frac{\partial \varphi_j}{\partial \zeta} \end{bmatrix}_{\zeta=0} \quad \text{where} \quad \mathbf{J}(\xi, \eta, \zeta) := \begin{bmatrix} \frac{\partial x^h}{\partial \xi} & \frac{\partial y^h}{\partial \xi} & \frac{\partial z^h}{\partial \xi} \\ \frac{\partial x^h}{\partial \eta} & \frac{\partial y^h}{\partial \eta} & \frac{\partial z^h}{\partial \eta} \\ \frac{\partial x^h}{\partial \zeta} & \frac{\partial y^h}{\partial \zeta} & \frac{\partial z^h}{\partial \zeta} \end{bmatrix},$$

This gives, at $\zeta = 0$,

$$\begin{bmatrix} \frac{\partial \varphi_i}{\partial x} \\ \frac{\partial \varphi_i}{\partial y} \\ \frac{\partial \varphi_i}{\partial z} \end{bmatrix} = \mathbf{J}^{-1}(\xi, \eta, 0) \begin{bmatrix} \frac{\partial \varphi_i}{\partial \xi} \\ \frac{\partial \varphi_i}{\partial \eta} \\ 0 \end{bmatrix}.$$

With the approximate normals we explicitly obtain

$$\left. \frac{\partial \mathbf{x}^h}{\partial \zeta} \right|_{\zeta=0} = \mathbf{n}^h,$$

so

$$\mathbf{J}(\xi, \eta, 0) := \begin{bmatrix} \frac{\partial x^h}{\partial \xi} & \frac{\partial y^h}{\partial \xi} & \frac{\partial z^h}{\partial \xi} \\ \frac{\partial x^h}{\partial \eta} & \frac{\partial y^h}{\partial \eta} & \frac{\partial z^h}{\partial \eta} \\ n_y^h & n_x^h & n_z^h \end{bmatrix}.$$

Remark 3.1 *The approach by Dziuk [12] (and also the classical engineering approach, [15]) is, in our setting, a constant-by-element extension of the geometry using facet triangles $\{T\}$ so that, with \mathbf{n}_T the normal to the facet, $\mathbf{x}^h(\xi, \eta, \zeta)|_T = \sum_i \mathbf{x}_i \varphi_i(\xi, \eta)|_T + \zeta \mathbf{n}_T$, and*

$$\begin{bmatrix} \frac{\partial \varphi_i}{\partial x} \\ \frac{\partial \varphi_i}{\partial y} \\ \frac{\partial \varphi_i}{\partial z} \end{bmatrix} = \mathbf{J}^{-1}(\xi, \eta, 0) \begin{bmatrix} \frac{\partial \varphi_i}{\partial \xi} \\ \frac{\partial \varphi_i}{\partial \eta} \\ 0 \end{bmatrix}, \quad \mathbf{J}(\xi, \eta, 0) := \begin{bmatrix} \frac{\partial x^h}{\partial \xi} & \frac{\partial y^h}{\partial \xi} & \frac{\partial z^h}{\partial \xi} \\ \frac{\partial x^h}{\partial \eta} & \frac{\partial y^h}{\partial \eta} & \frac{\partial z^h}{\partial \eta} \\ n_{Tx} & n_{Ty} & n_{Tz} \end{bmatrix}.$$

This low order approximation has the advantage of yielding a constant Jacobian from a linear approximation. For some applications this is, however, offset by the problem of having a discontinuous normal between elements.

3.2 Finite element formulation

We can now introduce finite element spaces constructed from the basis previously discussed by defining

$$W^h := \{v : v|_T \circ \mathbf{F} \in P^k(\hat{T}), \forall T \in \mathcal{T}_h; v \in C^0(\Sigma_h)\}, \quad (3.3)$$

(in the numerics, we use $k = 1$), and the finite element method reads: Find $\mathbf{u}_h \in V^h := [W^h]^3$ such that

$$a_{\Sigma_h}(\mathbf{u}_h, \mathbf{v}) = l_{\Sigma_h}(\mathbf{v}), \quad \forall \mathbf{v} \in V^h, \quad (3.4)$$

where

$$\begin{aligned} a_{\Sigma_h}(\mathbf{u}, \mathbf{v}) = & (2\mu \boldsymbol{\varepsilon}_{\Sigma_h}(\mathbf{u}), \boldsymbol{\varepsilon}_{\Sigma_h}(\mathbf{v}))_{\Sigma_h} - (4\mu \boldsymbol{\varepsilon}_{\Sigma_h}(\mathbf{u}) \cdot \mathbf{n}^h, \boldsymbol{\varepsilon}_{\Sigma_h}(\mathbf{v}) \cdot \mathbf{n}^h)_{\Sigma_h} \\ & + (\lambda_0 \nabla_{\Sigma_h} \cdot \mathbf{u}, \nabla_{\Sigma_h} \cdot \mathbf{v})_{\Sigma_h} \end{aligned}$$

and $l_{\Sigma_h}(\mathbf{v}) = (\mathbf{f}, \mathbf{v})_{\Sigma_h}$.

3.3 Extension to surfaces with a boundary

If the surface Σ has a boundary $\partial\Sigma$ we assume that $\partial\Sigma = \cup_i \partial\Sigma_i$ where $\partial\Sigma_i$ are closed components. On each of the components $\partial\Sigma_i$ we let $\mathbf{q}_j : \partial\Sigma_i \rightarrow \mathbf{R}^3, j = 1, 2, 3$, be smooth orthonormal vector fields. We strongly impose homogeneous Dirichlet boundary conditions of the type

$$\mathbf{q}_j \cdot \mathbf{u} = 0 \quad \text{on } \partial\Sigma_i, \quad 1 \leq j \leq d_i, \quad (3.5)$$

where $d_i = 1, 2$, or 3 , and weakly the remaining Neumann condition

$$(\mathbf{n}_{\partial\Sigma} \cdot \boldsymbol{\sigma}_{\Sigma}^P(\mathbf{u})) \cdot \mathbf{q}_j = 0, \quad d_i < j \leq 3, \quad (3.6)$$

where $\mathbf{n}_{\partial\Sigma}$ is the unit vector that is normal to $\partial\Sigma$ and tangent to Σ . Note that not every combination of boundary conditions and right hand side leads to a well posed problem.

4 Numerical examples

In the numerical examples below, the geometry is represented by flat facets, and the normals are taken as the exact normal in the nodes, interpolated linearly inside each element. Our experience is that similar results are obtained if we use L_2 -projections of the flat facet normals in the nodes and then interpolate these linearly.

4.1 Pulling a cylinder

We consider a cylindrical shell of radius r and thickness t , with open ends at $x = 0$ and at $x = L$, and with fixed longitudinal displacements at $x = 0$, and radial at $x = L$, carrying a horizontal surface load per unit area

$$f(x, y, z) = \frac{F}{2\pi r} \frac{x}{L^2},$$

where F has the unit of force. The resulting longitudinal stress is

$$\sigma = \frac{F(1 - (x/L)^2)}{4\pi r t}.$$

We take as an example a cylinder of radius $r = 1$ and length $L = 4$, with material data $E = 100$ and $\nu = 1/2$, with thickness $t = 10^{-2}$, and with $F = 1$. In Fig. 1 we show the solution (exaggerated 10 times) on a particular mesh (shown in Fig. 2). Note that the lateral contraction creates radial displacements depending on the size of stress. Finally, in Fig. 3 we show the L_2 error in stresses, $\|\boldsymbol{\sigma} - \boldsymbol{\sigma}_h\|_{L_2(\Omega)}$, where $\boldsymbol{\sigma} := \boldsymbol{\sigma}_\Sigma^P(\mathbf{u})$ and $\boldsymbol{\sigma}_h := \boldsymbol{\sigma}_\Sigma^P(\mathbf{u}_h)$, which shows the expected first order convergence for our P^1 approximation. The black triangle shows the 1:1 slope.

4.2 A torus with internal pressure

We consider a torus with internal gauge pressure p for which the stresses are statically determinate. Using the angle and radii defined in Fig. 4, the principal stresses are given by

$$\sigma_1 = \frac{pr}{2t}, \quad \sigma_2 = \frac{pr}{t} \left(1 - \frac{r \sin \theta}{2(R + r \sin \theta)} \right),$$

where σ_1 is the longitudinal stress, σ_2 the hoop stress, and t is the thickness of the surface of the torus. The constitutive parameters and thickness were chosen as in the cylinder example, and we set $R = 1$, $r = 1/2$, and $p = 1$.

Again we compute the stress error $\|\boldsymbol{\sigma} - \boldsymbol{\sigma}_h\|_{L_2(\Omega)}$. We show the observed convergence in Fig. 7 at a rate of about 3/4 (the slope of the black triangle), which is suboptimal, but does occur in problems where elliptic regularity is an issue, cf. [3], Lemma 10. We thus attribute this loss of convergence to the load now being in the normal direction of the shell, for which we do not have ellipticity.

References

- [1] E. Bänsch, P. Morin, and R. H. Nochetto. Surface diffusion of graphs: variational formulation, error analysis, and simulation. *SIAM J. Numer. Anal.*, 42(2):773–799, 2004.
- [2] J. W. Barrett, H. Garcke, and T. Nürnberg. On the parametric finite element approximation of evolving hypersurfaces in \mathbb{R}^3 . *J Comput. Phys.*, 227(9):4281 – 4307, 2008.
- [3] E. Burman and P. Hansbo. Edge stabilization for Galerkin approximations of convection-diffusion-reaction problems. *Comput. Methods Appl. Mech. Engrg.*, 193(15-16):1437–1453, 2004.

- [4] P. G. Ciarlet. *Mathematical elasticity. Vol. III: Theory of shells*, volume 29 of *Studies in Mathematics and its Applications*. North-Holland Publishing Co., Amsterdam, 2000.
- [5] P. G. Ciarlet and V. Lods. Asymptotic analysis of linearly elastic shells. I. Justification of membrane shell equations. *Arch. Rational Mech. Anal.*, 136(2):119–161, 1996.
- [6] P. G. Ciarlet and É. Sanchez-Palencia. Un théorème d’existence et d’unicité pour les équations des coques membranaires. *C. R. Acad. Sci. Paris Sér. I Math.*, 317(8):801–805, 1993.
- [7] K. Deckelnick, G. Dziuk, C. M. Elliott, and C.-J. Heine. An h -narrow band finite-element method for elliptic equations on implicit surfaces. *IMA J. Numer. Anal.*, 30(2):351–376, 2010.
- [8] M. C. Delfour and J.-P. Zolésio. A boundary differential equation for thin shells. *J. Differential Equations*, 119(2):426–449, 1995.
- [9] M. C. Delfour and J.-P. Zolésio. Tangential differential equations for dynamical thin/shallow shells. *J. Differential Equations*, 128(1):125–167, 1996.
- [10] M. C. Delfour and J.-P. Zolésio. Differential equations for linear shells: comparison between intrinsic and classical models. In *Advances in mathematical sciences: CRM’s 25 years (Montreal, PQ, 1994)*, volume 11 of *CRM Proc. Lecture Notes*, pages 41–124. Amer. Math. Soc., Providence, RI, 1997.
- [11] A. Demlow and G. Dziuk. An adaptive finite element method for the Laplace-Beltrami operator on implicitly defined surfaces. *SIAM J. Numer. Anal.*, 45(1):421–442, 2007.
- [12] G. Dziuk. Finite elements for the Beltrami operator on arbitrary surfaces. In *Partial differential equations and calculus of variations*, volume 1357 of *Lecture Notes in Math.*, pages 142–155. Springer, Berlin, 1988.
- [13] C. M. Elliott and B. Stinner. Modeling and computation of two phase geometric biomembranes using surface finite elements. *J Comput. Phys.*, 229(18):6585 – 6612, 2010.
- [14] M. A. Olshanskii, A. Reusken, and J. Grande. A finite element method for elliptic equations on surfaces. *SIAM J. Numer. Anal.*, 47(5):3339–3358, 2009.
- [15] O. C. Zienkiewicz. *The finite element method in engineering science*. McGraw-Hill, London, 1971.

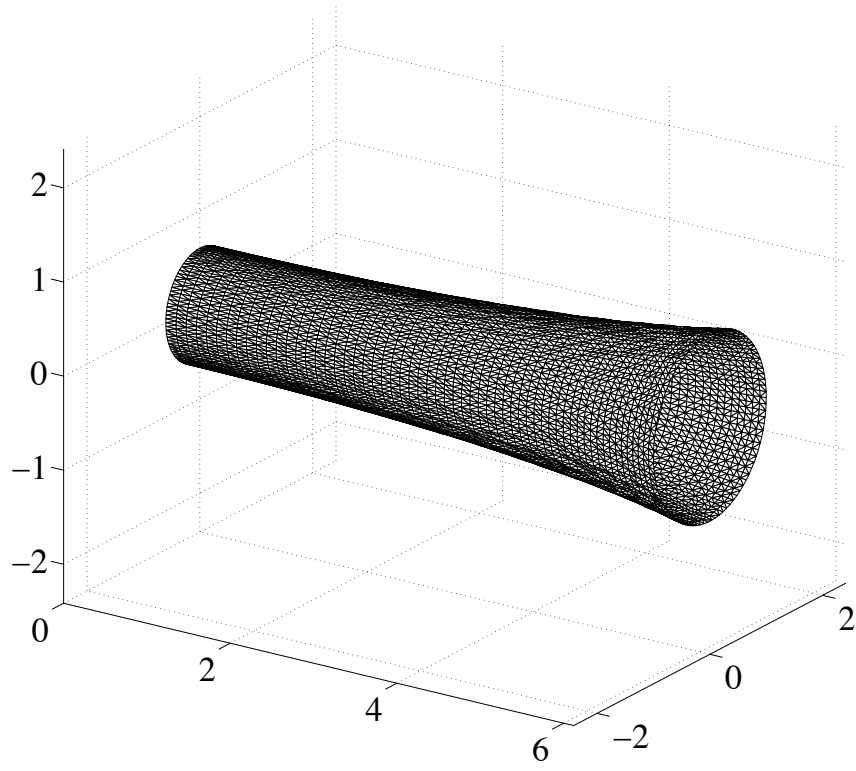


Figure 1: Displacements (exaggerated by one order of magnitude) on a particular mesh.

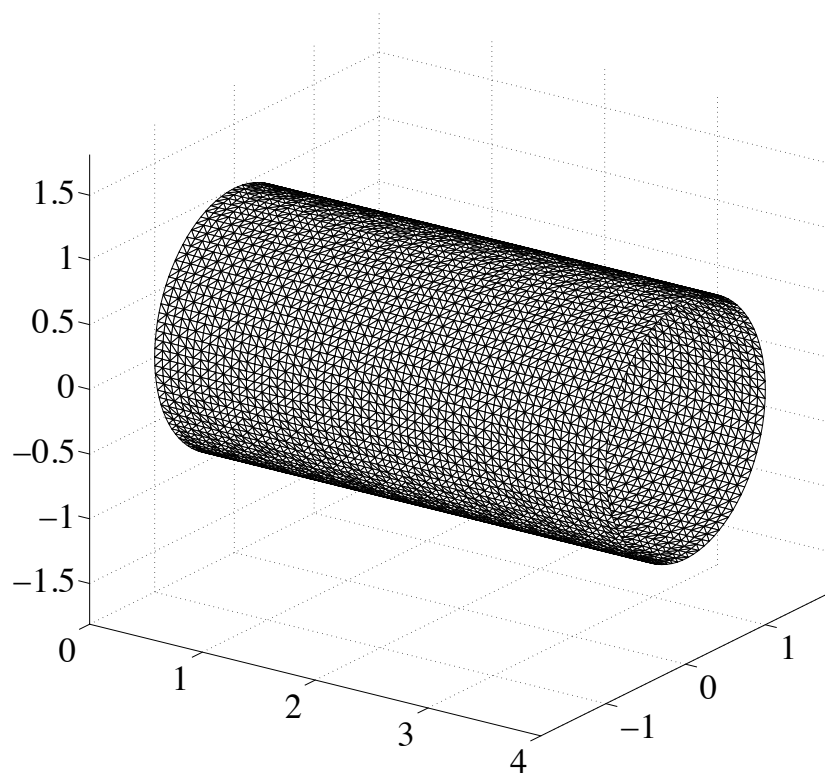


Figure 2: The cylinder before deformation.

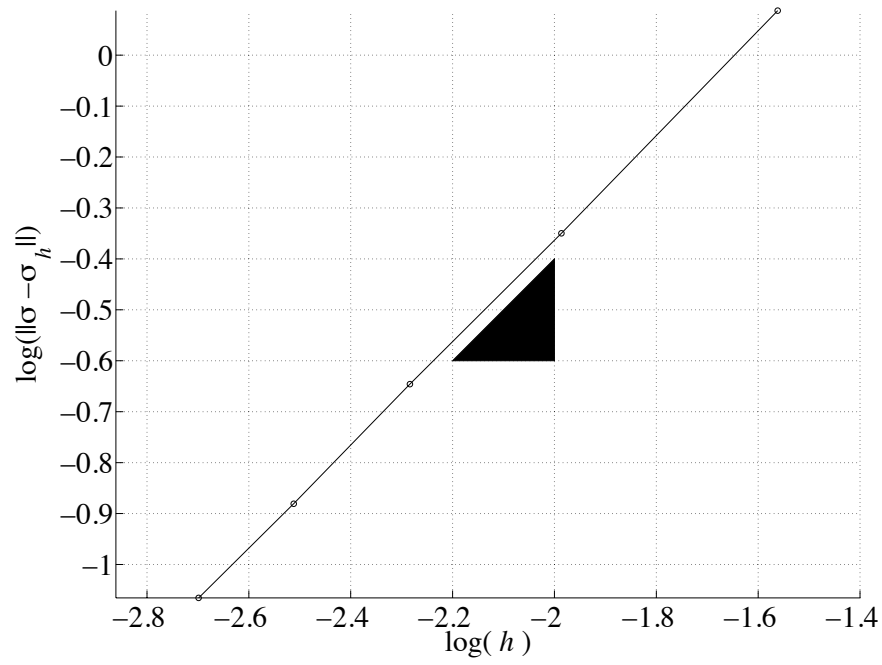


Figure 3: Stress convergence for the cylinder

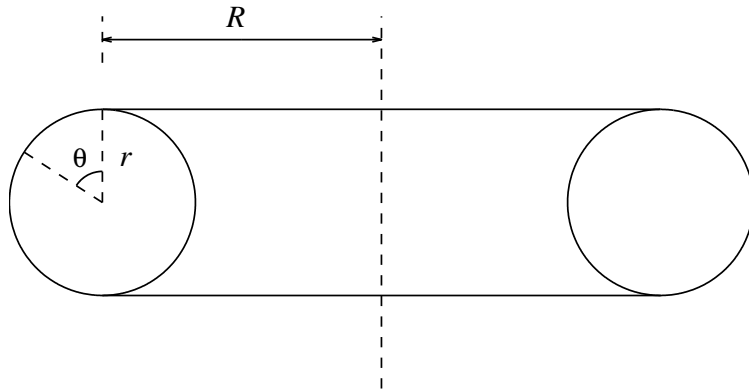


Figure 4: A cut through of the torus

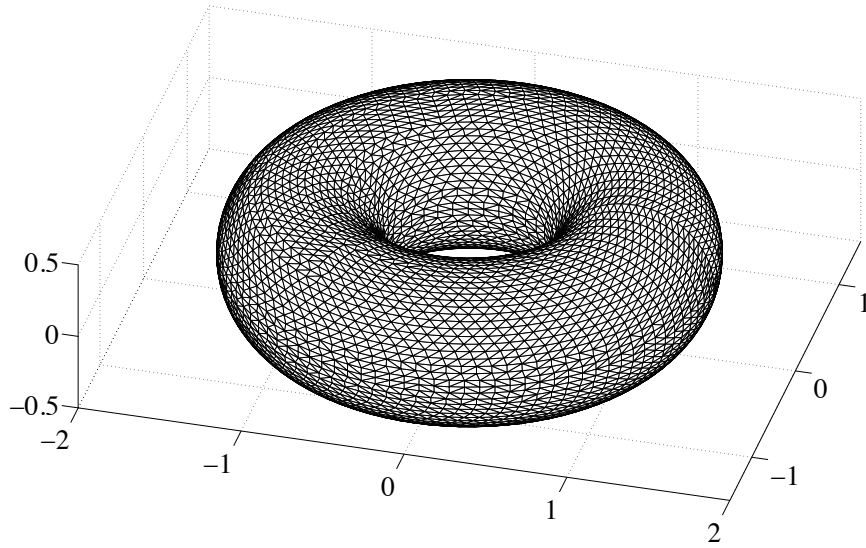


Figure 5: A typical mesh on the torus.

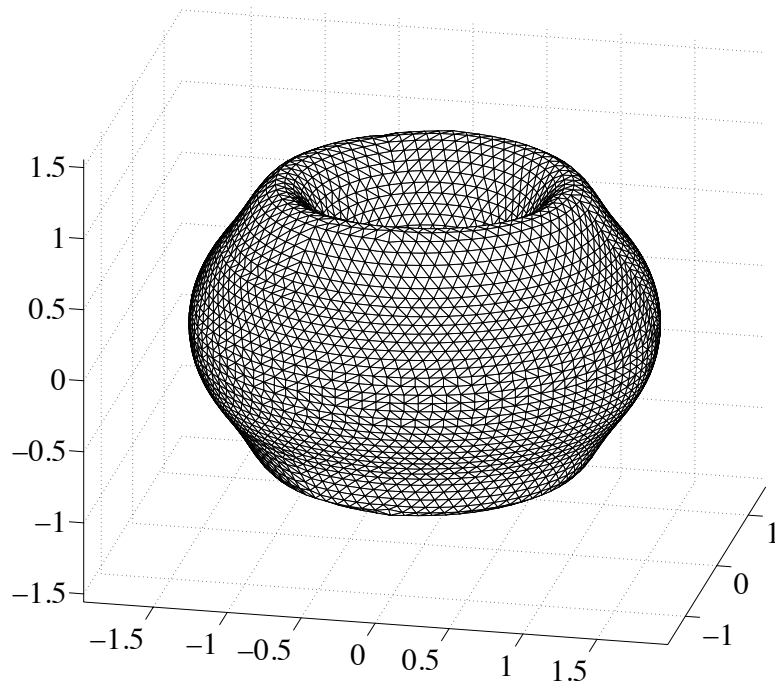


Figure 6: Deformations in the torus case, exaggerated by two orders of magnitude.

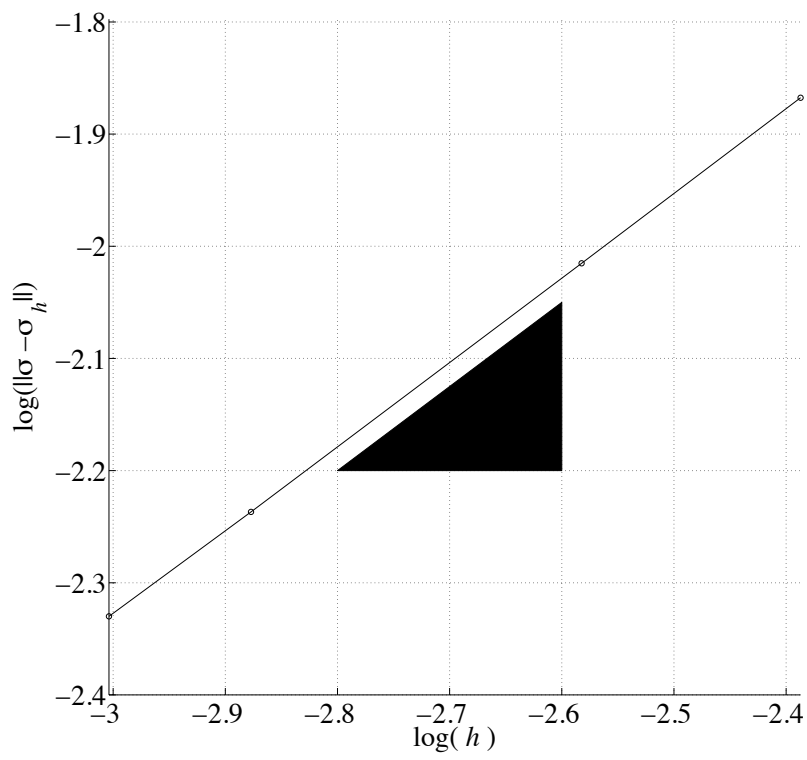


Figure 7: Convergence of the stresses in the torus case.